

Effect of Void Network on CMB AnisotropyNobuyuki Sakai^{1*}, Naoshi Sugiyama², and Jun'ichi Yokoyama¹¹Yukawa Institute for Theoretical Physics, Kyoto University, Kyoto 606-8502, Japan²Department of Physics, Kyoto University, Kyoto 606-8502, Japan**ABSTRACT**

We study the effect of a void network on the CMB anisotropy in the Einstein-de Sitter background using Thompson & Vishniac's model. We consider comprehensively the Sacks-Wolfe effect, the Rees-Sciama effect and the gravitational lensing effect. Our analysis includes the model of primordial voids existing at recombination, which is realized in some inflationary models associated with a first-order phase transition. If there exist primordial voids whose comoving radius is larger than $\sim 10h^{-1}\text{Mpc}$ at recombination, not only the Sachs-Wolfe effect but also the Rees-Sciama effect is appreciable even for multipoles $l \lesssim 1000$ of the anisotropy spectrum. The gravitational lensing effect, on the other hand, slightly smoothes the primary anisotropy; quantitatively, our results for the void model are similar to the previous results for a CDM model. All the effects, together, would give some constraints on the configuration or origin of voids with high-resolution data of the CMB anisotropy.

Subject headings: cosmic microwave background, large scale structure

1. Introduction

The anisotropy of the cosmic microwave background (CMB) is an important probe of primordial fluctuations at recombination, which carries information on the cosmological parameters as well as the nature of dark matter (see, e.g., Hu, Sugiyama & Silk 1997). CMB photons, however, are also affected gravitationally by nonlinear structures between recombination and the present epoch. In fact, a network of voids filling the entire universe has been suggested by redshift surveys such as the CfA2 (Geller & Huchra 1989) and the SSRS2 (da Costa et al. 1994). Moreover, using such redshift surveys, El-Ad, Piran & da Costa (1996, 1997) and El-Ad & Piran (1997) quantified voids in the galaxy distribution and confirmed the description of a void-filled universe: they showed that $\sim 50\%$ of the volume is filled with the voids and that the voids have a

*E-mail: sakai@yukawa.kyoto-u.ac.jp

diameter of at least $40h^{-1}\text{Mpc}$ with an average underdensity of -0.9 . In this paper we investigate the effect of a void network on the CMB anisotropy in the Einstein-de Sitter background.

Rees and Sciama (1968, hereafter RS) showed that an evolving nonlinear structure perturbs the redshift of a photon passing through it by use of the “Swiss-cheese” model of overdensity. Later Thompson & Vishniac (1987, hereafter TV) estimated this RS effect in a void network model. First, they considered a spherical void in the Einstein-de Sitter background and derived an analytic expression of the redshift deviation $\delta T/T$ under the thin-shell approximation. Then, using this expression of $\delta T/T$, they calculated the variance of $\delta T/T$ for a universe filled with voids. As we will review in §2, the CMB anisotropy produced by the void network is of the order 10^{-6} if the present diameter of all voids is $60h^{-1}\text{Mpc}$ and if they have formed at $z < 10$; if the formation time is earlier, the anisotropy becomes larger. These results were supported by several authors (Sato 1985; Martínez-González, Sanz & Silk 1990; Martínez-González & Sanz 1990; Mészáros 1994; Mészáros & Molnár 1996; Panek 1992; Arnau, Fullana & Monreal 1993; Fullana, Arnau & Saez 1996; Shi, Widrow & Dursi 1996). Although density perturbations are usually assumed to be linear at the last-scattering surface (LSS), nonlinear voids can exist there if voids are originated by primordial bubbles which are nucleated in a phase transition during inflation (La 1991; Liddle & Wands 1991; Turner, Weinberg & Widrow 1992; Occhionero & Amendola 1994; Amendola et al. 1996; Baccigalupi, Amendola & Occhionero 1997; Baccigalupi et al. 1997; Amendola, Baccigalupi, & Occhionero 1998; Baccigalupi 1998). Although the hypothesis of primordial voids is quite different from conventional scenarios, it may explain the present void-network structure and deserves further consideration. Therefore, more quantitative analysis of the RS effect for that case is important. One of the purposes of the present analysis is to calculate the power spectrum of the CMB anisotropy by extending TV’s analysis.

The lensing effect of density perturbations, on the other hand, has also been investigated by several authors (Blanchard & Schneider 1987; Kashlinsky 1988; Cole & Efstathiou 1989; Sasaki 1989; Tomita 1989; Tomita & Watanabe 1989; Fukushige, Makino & Ebisuzaki 1994; Linder 1990a, b; Cayón, Martínez-González & Sanz 1993a, b; Seljak 1996; Martínez-González, Sanz & Cayón 1997). It has been concluded, as a whole, that the effect is appreciable on arcminute angular scales for some models while it is negligible on degree scales. In particular, Seljak (1996) solved the shortcomings of the previous studies to include the nonlinear effects by modeling the power spectrum evolution in the nonlinear regime, and Martínez-González, Sanz & Cayón (1997) extended his method to study more general models; it was shown (Seljak 1996; Martínez-González, Sanz & Cayón 1997) that for a CDM model the lensing effect changes the CMB angular power spectrum C_l considerably for $l \gtrsim 1000$. This power spectrum approach can be applied to general models as long as the power spectrum of density perturbations is known. Because the power spectrum of a void-network universe is not obtained, however, we shall estimate the lensing effect in a different way. That is, we estimate the correction of the primary anisotropy, using TV’s formula of the scattering angle of a photon by a void. An advantage of our approach is that we make no approximation for nonlinearity nor relativistic effect.

In case nonlinear voids already exist at recombination — which is the case we are most interested in — we should also include the Sachs-Wolfe (1967, hereafter SW) effect of voids sitting on the LSS. In fact, it has been investigated by Baccigalupi, Amendola & Occhionero (1997), Amendola, Baccigalupi & Occhionero (1998), and Baccigalupi (1998) to constrain an inflationary model; it has been shown that the maximum radius allowed by the COBE data is $\approx 25h^{-1}\text{Mpc}$ on the LSS, and that its non-Gaussianity is large enough to be observable. In their analysis they have ignored the RS term by comparing both terms for a single void. We agree to their conclusions as a whole, but it is not clear whether the total contribution is also negligible because the RS effect is generated not by a single void but by multiple voids between the LSS and us. Further, the lensing effect of such voids is also unclear. We thus consider the effect of a void network, taking account of the RS effect and the lensing effect as well as the SW effect.

The plan of this paper is as follows. In §2, we briefly review TV’s model and results, which we extend in the following sections. In §3, we apply the potential approximation to estimate the SW term. In §4, we calculate the anisotropy spectra for the RS effect and for the SW effect of a void network. In §5, we investigate how the primordial fluctuations are modified by the gravitational lensing effect of a void network. §6 is devoted to summary and discussions.

2. Rees-Sciama Effect — Thompson & Vishniac’s Model and Results —

Because our analysis is based on TV’s model of a void-network universe and their analytical results, here we review them briefly. Consider a single spherical void in the Einstein-de Sitter background:

$$ds^2 = -dt^2 + a^2(t)(dr^2 + r^2d\theta^2 + r^2\sin^2\theta d\varphi^2) \quad \text{with} \quad a(t) = \left(\frac{t}{t_0}\right)^{\frac{2}{3}}, \quad (1)$$

where t_0 is the present time. The void itself is an empty spherical region, and hence a Minkowski spacetime:

$$ds^2 = -dt'^2 + dx'^2 + x'^2d\theta^2 + x'^2\sin^2\theta d\varphi^2, \quad (2)$$

where the prime denotes an internal coordinate. The matter surrounding a void is assumed to form a thin shell. From momentum conservation and energy conservation, respectively, Maeda & Sato (1983) and Bertschinger (1985) showed that the shell radius expands asymptotically as

$$r_v(t) \propto t^\beta \quad \text{with} \quad \beta \approx 0.13. \quad (3)$$

Figure 1 shows TV’s model of a photon passing through a spherical void. The subscripts 1 and 2 denote quantities at the time the photon enters the void and at the time it leaves, respectively. We define α as the angle formed between the direction of observation and the direction of the void’s center, $\delta\alpha$ as the scattering angle of a photon, d as the comoving distance of the void’s center, and d_{LSS} as the comoving distance of the LSS. The angles ψ_1 , ψ'_1 , ψ'_2 and ψ_2 are defined by reference to Figure 1.

TV applied double local Lorentz transformations at each void boundary. For example, the relation between the momentum vector just before entering a void, \mathbf{k}_1 , and the one just after passing the shell, \mathbf{k}'_1 , is expressed as

$$\mathbf{k}_1 \equiv E_1 \begin{pmatrix} 1 \\ \cos \psi_1 \\ \sin \psi_1 \\ 0 \end{pmatrix}, \quad (4)$$

$$\mathbf{k}'_1 \equiv E'_1 \begin{pmatrix} 1 \\ \cos \psi'_1 \\ \sin \psi'_1 \\ 0 \end{pmatrix} = E_1 \begin{pmatrix} \gamma_1 \gamma'_1 [1 + (v_1 - v'_1) \cos \psi_1 - v_1 v'_1] \\ \gamma_1 \gamma'_1 [\cos \psi_1 + (v_1 - v'_1) - v_1 v'_1 \cos \psi_1] \\ \sin \psi_1 \\ 0 \end{pmatrix}, \quad (5)$$

where velocities and Lorentz factors are defined as

$$v_1 \equiv a \frac{dr_v}{dt} \Big|_{t=t_1}, \quad v'_1 \equiv \frac{d(ar_v)}{dt'} \Big|_{t=t_1}, \quad \gamma_1 \equiv \frac{1}{\sqrt{1-v_1^2}}, \quad \gamma'_1 \equiv \frac{1}{\sqrt{1-v'^2_1}}. \quad (6)$$

In Appendix A we show the equations of the ‘‘Lorentz transformation’’ can be derived exactly from a general coordinate transformation in a curved spacetime.

After lengthy algebraic calculations, one obtains the redshift deviation and the scattering angle of a photon:

$$\frac{\delta T}{T} = (H_2 R_2)^3 \cos \psi_2 \left(3\beta - \frac{2}{3} \cos^2 \psi_2 \right) \equiv \Delta_{\text{RS}}, \quad (7)$$

$$\delta \alpha \equiv -\psi_1 + \psi'_1 + \psi'_2 - \psi_2 = (H_2 R_2)^2 \sin(2\psi_2), \quad (8)$$

where H is the Hubble parameter, and $R \equiv ar_v$ is the proper length of the shell radius.

Next, TV estimated the CMB anisotropy produced by a void network. Their model consists of randomly distributed, equally sized, and non-overlapped voids, which formed at some time t_f simultaneously. Divide the universe into shells of the comoving thickness $2r_v(t_0)$, as depicted in Figure 2. For each shell, the probability of a ray intersecting a void is given by

$$P = \frac{3}{2} F_0 \left(\frac{t}{t_0} \right)^{2\beta}, \quad (9)$$

where F_0 is the fractional volume of space occupied by voids and normalized at the present. The variance of $\delta T/T$ for each shell is

$$\sigma_{\text{RS,shell}}^2 \equiv \langle \Delta_{\text{RS}}^2 \rangle_{\text{shell}} - \langle \Delta_{\text{RS}} \rangle_{\text{shell}}^2, \quad (10)$$

where

$$\langle \Delta_{\text{RS}}^2 \rangle_{\text{shell}} = P \int_0^{\frac{\pi}{2}} \Delta_{\text{RS}}^2 \sin \psi_2 d\psi_2, \quad (11)$$

and Δ is given by equation (7). Strictly speaking, the integration should be performed with respect to α instead of ψ_2 . However, unless a void is very close to an observer, ψ_2 is almost proportional to α , and hence the integration (11) is a good approximation.

The net variance is

$$\sigma_{\text{RS}}^2 = \sum \sigma_{\text{RS,shell}}^2, \quad (12)$$

where the sum is over all the shells from t_f to t_0 . We can approximate it with an integral

$$\sigma_{\text{RS}}^2 = \int_{t_f}^{t_0} \sigma_{\text{RS,shell}}^2 \frac{dt}{\Delta t} \quad \text{with} \quad \Delta t \equiv 2a(t)r_v(t_0). \quad (13)$$

After an algebraic calculation, we obtain

$$\begin{aligned} \sigma_{\text{RS}} = & \frac{3}{2}(H_0 R_0)^{\frac{5}{2}} \left[\frac{3F_0}{5-24\beta} \left(\frac{2}{81} - \frac{8}{27}\beta + \beta^2 \right) \left\{ (1+z_f)^{\frac{5}{2}-12\beta} - 1 \right\} \right. \\ & \left. - \frac{4F_0^2}{5(1-6\beta)} \left(\beta - \frac{2}{15} \right)^2 \left\{ (1+z_f)^{\frac{5}{2}-15\beta} - 1 \right\} \right]^{\frac{1}{2}}. \end{aligned} \quad (14)$$

TV mentioned that the second term in equation (14) goes to zero if $\beta = 2/15$ (≈ 0.133), or equivalently, $\langle \Delta_{\text{RS}} \rangle = 0$. Although we take Maeda & Sato's result $\beta = 0.13$ throughout this paper, $\langle \Delta_{\text{RS}} \rangle \approx 0$ is still satisfied.

In the present model there are three parameters: the radius of voids R_0 , the volume fraction F_0 , and the formation time z_f . z_f should be $1 \sim 10$ in conventional scenarios of structure formation, while $z_f = z_{\text{LSS}} \approx 1000$ in the scenario that voids are originated by primordial bubbles at the inflationary era. As for R_0 and F_0 , we consider three cases:

- (i). $R_0 = 20h^{-1}\text{Mpc}$ and $F_0 = 60\%$.
- (ii). $R_0 = 30h^{-1}\text{Mpc}$ and $F_0 = 60\%$.
- (iii). $R_0 = 60h^{-1}\text{Mpc}$ and $F_0 = 3\%$.

It must be noted that voids are not at rest in terms of the comoving coordinates but expands with the power law in equation (3). Therefore, for example, a void with $R_0 = 60h^{-1}\text{Mpc}$ at present corresponds to a void with the comoving radius $r_v(t_{\text{LSS}}) \approx 15h^{-1}\text{Mpc}$ on the LSS. Models (i) and (ii) are based on the analysis of redshift surveys by El-Ad et al. (1996, 1997) and El-Ad & Piran (1997), which we introduced in §1. In the real Universe, however, voids should have a smooth distribution function in size, and a small number of much larger voids may affect the CMB anisotropy. Therefore, we also consider Model (iii), as an example. Later our result (in Fig. 8(c)) will show that Model (iii) is compatible with COBE's data. As we mentioned in §1, Baccigalupi, Amendola & Occhionero (1997) also considered such large voids, and showed that the maximum radius is $\approx 25h^{-1}\text{Mpc}$ on the LSS, which corresponds to $\approx 100h^{-1}\text{Mpc}$ at present, from the compatibility between the SW effect of voids and COBE's data.

To illustrate the typical values of σ_{RS} , we draw a plot of equation (14) in Figure 3. We see that the net variance depends strongly on the formation time of voids. As TV concluded, the RS effect cannot make a dominant contribution to the CMB anisotropy if nonlinear voids form at $z < 10$. On the other hand, if voids form before or just after recombination (i.e., $z_f \approx 1000$), the RS effect may not be negligible.

3. Sachs-Wolfe Effect — Estimate with Potential Approximation —

As we mentioned in the introduction, for the case where the primordial voids exist already at recombination, the SW effect by those voids should be taken into account. First, we estimate the SW effect of a single void, using the “potential approximation” devised by Martínez-González et al. (1990).

Even if the density profiles are nonlinear, under some condition the metric perturbations in the Einstein-de Sitter background are characterized by a single potential $\phi(t, \mathbf{x}) \ll 1$:

$$ds^2 = -(1 + 2\phi)dt^2 + (1 - 2\phi)a^2(t)(dr^2 + r^2d\theta^2 + r^2\sin^2\theta d\varphi^2), \quad (15)$$

and the energy-momentum tensor by the matter density $\rho(t, \mathbf{x})$ and the velocity field $\mathbf{v}(t, \mathbf{x})$. Then one of the Einstein equations reduces to the Poisson equation:

$$\frac{1}{a^2} \Delta \phi = 4\pi G \rho_b \frac{\delta\rho}{\rho}, \quad (16)$$

where ρ_b is the background density and $\delta\rho/\rho$ is the density fluctuation field: $\rho = \rho_b(1 + \delta\rho/\rho)$. Martínez-González et al. (1990) derived the general expression of redshift fluctuations:

$$\frac{\delta T}{T} = \frac{1}{3}(\phi_{\text{LSS}} - \phi_0) - 2 \int_{\text{LSS}}^0 d\mathbf{x} \cdot \nabla \phi + \mathbf{n} \cdot (\mathbf{v}_0 - \mathbf{v}_{\text{LSS}}). \quad (17)$$

The first, the second, and the third terms are interpreted as the SW effect, the RS effect, and the Doppler effect, respectively. They also showed that, for an empty void, the second term results in equation (7), which is TV’s result.

Let us calculate the potential inside a void. For a spherical void with a thin shell, $\rho(t, \mathbf{x})$ is explicitly written as

$$\rho(t, r) = \rho_b(t)\theta(r - r_v(t)) + \rho_{\text{in}}(t, r)\theta(r - r_v(t)) + \sigma(t)\delta_{\text{Dirac}}(r - r_v(t)), \quad (18)$$

where θ is the Heviside function, δ_{Dirac} is Dirac’s delta function, ρ_{in} is the energy density inside the void, and σ is the surface energy density of the shell. If we assume ρ_{in} to be homogeneous, the Poisson equation (16) is easily integrated as

$$\phi = \frac{1}{4}H^2a^2(r^2 - r_v^2)\frac{\delta\rho}{\rho}, \quad \text{for } r < r_v, \quad (19)$$

and $\phi = 0$ for $r > r_v$. This result is also obtained in the usual linear perturbation theory. What we want to emphasize here is, however, that equation (19) can also be applied to nonlinear density profiles such as the present void model. For an empty void ($\delta\rho/\rho = -1$ for $r < r_v$), assuming $\phi_0 = 0$, we obtain the temperature distortion by the SW effect,

$$\frac{\delta T}{T} = \frac{1}{12} H^2 a^2 (r_v^2 - r^2)|_{\text{LSS}}, \quad (20)$$

which takes a maximal value at $r = 0$, corresponding to the case where the void's center is just located on the LSS, and vanishes for $r > r_v$. In order to take an average over the the location of voids within the farthest shell, we define X as the distance between the void's center and the LSS (see Fig. 4) and rewrite equation (20) as

$$\frac{\delta T}{T} = \frac{1}{12} H^2 a^2 (r_v^2 \cos^2 \psi_2 - X^2) \equiv \Delta_{\text{SW}}. \quad (21)$$

The variance of $\delta T/T|_{\text{SW}}$ is calculated as

$$\sigma_{\text{SW}}^2 \equiv \langle \Delta_{\text{SW}}^2 \rangle - \langle \Delta_{\text{SW}} \rangle^2, \quad (22)$$

where

$$\langle \Delta_{\text{SW}}^2 \rangle = P \int_0^{\frac{\pi}{2}} \sin \psi_2 d\psi_2 \left[\frac{1}{r_0} \int_0^{r_v \cos \psi_2} dX \Delta_{\text{SW}}^2 \right]. \quad (23)$$

Figure 5 shows a plot of equations (23) with a plot of (14). As long as we look at the variance of temperature fluctuations, both terms seem to make comparable contributions. The next task is, of course, to investigate scale-dependent properties of both effects.

4. Rees-Sciama Effect and Sachs-Wolfe Effect — Calculation of C_l —

For TV's model of a void network, we shall calculate the angular correlation functions of the CMB anisotropy $C(\theta)$ for the RS term and for the SW term, and their multipole moments C_l , which are defined by

$$C(\theta) \equiv \left\langle \frac{\delta T}{T}(\boldsymbol{\theta}_A) \frac{\delta T}{T}(\boldsymbol{\theta}_B) \right\rangle_{\theta} \equiv \sum_l \frac{(2l+1)C_l}{4\pi} P_l(\cos \theta), \quad (24)$$

where $\boldsymbol{\theta}_A$ and $\boldsymbol{\theta}_B$ are angular positions with the separation angle θ .

First, let us consider the RS effect. In general, in order to calculate the correlation function with density configuration in a real space, simulation-like computation is needed. Once we evaluate $C_{\text{RS}}(\theta)$ for each shell, however, we can sum up the contributions from all shells by using the same relation as equation (12). Furthermore, for each shell, by the assumption of random distribution of voids and by the relation $\langle \Delta_{\text{RS}} \rangle \approx 0$, the correlation function $C_{\text{RS}}(\theta)$ for the case where two light rays A and B pass different voids becomes zero; this allows us to consider only one void in

our calculation. Let us imagine a void projected on the celestial sphere, as depicted in Figure 6. The angles α_A , α_B , α_c , α_s , and ξ are defined by reference to Figure 6. We calculate $C_{\text{RS}}(\theta)$ for each shell by neglecting the curvature of the sphere in a local region around a void. Defining the midpoint of θ_A and θ_B as

$$\theta_c \equiv \frac{\theta_A + \theta_B}{2} = (\alpha_c, 0), \quad (25)$$

the positions of θ_A and θ_B are written as

$$\theta_A = \left(\alpha_c + \frac{\theta}{2} \cos \xi, \frac{\theta}{2} \sin \xi \right), \quad \theta_B = \left(\alpha_c - \frac{\theta}{2} \cos \xi, -\frac{\theta}{2} \sin \xi \right). \quad (26)$$

Then we can calculate $C_{\text{RS}}(\theta)$ for each shell with the expression

$$C_{\text{RS,shell}}(\theta) = \frac{\alpha_m^2}{\alpha_s^2} P \frac{2}{\alpha_m^2} \int_0^{\alpha_m} \alpha_c d\alpha_c \left[\frac{1}{\pi} \int_0^\pi d\xi \Delta_{\text{RS}}(\alpha_A) \Delta_{\text{RS}}(\alpha_B) \right], \quad (27)$$

where the relation between ψ_2 and α (α_A or α_B) is

$$\sin \psi_2 = \frac{d}{r_2} \sin \alpha \quad \text{with} \quad d = 3t_0 \left[1 - \left(\frac{t}{t_0} \right)^{\frac{1}{3}} \right], \quad (28)$$

and the angular size α_s which corresponds to the void radius and the integral boundary α_m are defined as

$$\alpha_s \equiv \alpha|_{\psi_2=\frac{\pi}{2}} = \arcsin \left(\frac{r_2}{d} \right), \quad \alpha_m \equiv \alpha_s + \frac{\theta}{2}. \quad (29)$$

The correlation function for the SW effect is calculated similarly: $C_{\text{SW}}(\theta)$ is given by

$$C_{\text{SW}}(\theta) = \frac{\alpha_m^2}{\alpha_s^2} P \frac{2}{\alpha_m^2} \int_0^{\alpha_m} \alpha_c d\alpha_c \left\{ \frac{1}{\pi} \int_0^\pi d\xi \left[\frac{1}{r_0} \int_0^{X(\Delta_{\text{SW}}=0)} dX \Delta_{\text{SW}}(\alpha_A) \Delta_{\text{SW}}(\alpha_B) \right] \right\}, \quad (30)$$

where $\Delta(\alpha)$ has been redefined as $\Delta(\alpha) - \langle \Delta(\alpha) \rangle \rightarrow \Delta(\alpha)$ so that $\langle \Delta(\alpha) \rangle = 0$.

Numerical integration of equations (27) and (30) gives us $C_{\text{RS}}(\theta)$ and $C_{\text{SW}}(\theta)$, and their multipole moments are obtained from

$$C_l = 2\pi \int_{-1}^1 C(\theta) P_l(\cos \theta) d(\cos \theta), \quad (31)$$

which are equivalent to equation (24).

Figure 7 reports how the anisotropy spectrum of the RS effect depends on the formation time z_f . Here we plot $\sqrt{l(l+1)}C_l$ versus $\log l$ in accordance with Amendola, Baccigalupi & Occhionero (1998). As we expected, the RS effect for $z_f = 10$ is negligibly small while it is not for $z_f = 1000$.

In Figure 8 we compare the RS effect and the SW effect for our three models. In Model (i) the RS effect is negligibly small; in Model (ii) it is still smaller than the SW effect for $l < 1000$, but it is more than 10% of the SW term for $l \lesssim 1000$ and not negligible; in Model (iii) both terms are comparable. The dependence of C_l on F_0 is easily understood: as equation (14) indicates, $\delta T/T$ or C_l is proportional to $\sqrt{F_0}$.

5. Gravitational Lensing Effect

We now turn to the lensing effect. First, we estimate the characteristic angular scale below which the lensing effect is appreciable, by calculating the angular excursion of a photon on the LSS, $\delta\theta$. The lens equation for a single void in the thin lens approximation is

$$\delta\theta_{\text{one void}} = W\delta\alpha\mathbf{l} \quad \text{with} \quad W \equiv \frac{d_{\text{LSS}} - d \cos \alpha}{d_{\text{LSS}}}, \quad (32)$$

where the vector $\mathbf{l} \equiv \delta\theta/|\delta\theta|$ has been introduced in Figure 1. In reality this thin lens equation can be derived exactly from null geodesic equations, as shown in Appendix B.

Replacing $\delta T/T$ with $W\delta\alpha$ in TV's calculation of σ_{RS} in §2, we find

$$\begin{aligned} \sqrt{\langle |\delta\theta|^2 \rangle} &= (H_0 R_0)^{\frac{3}{2}} \frac{\sqrt{F_0}}{\sqrt{z_{\text{LSS}} + 1} - 1} \left[\frac{1}{3(6\beta - 1)} - \frac{\sqrt{z_{\text{LSS}} + 1}}{9\beta - 1} + \frac{z_{\text{LSS}} + 1}{18\beta - 1} \right. \\ &\quad \left. - (z_f + 1)^{\frac{3}{2} - 9\beta} \left\{ \frac{1}{3(6\beta - 1)} - \sqrt{\frac{z_{\text{LSS}} + 1}{z_f + 1}} \frac{1}{9\beta - 1} + \frac{z_{\text{LSS}} + 1}{z_f + 1} \frac{1}{18\beta - 1} \right\} \right]^{\frac{1}{2}}. \end{aligned} \quad (33)$$

We draw a plot of equation (33) in Figure 9, assuming $z_{\text{LSS}} = 1000$. The lensing effect also depends on the formation time of voids, though the dependence is not so strong as in the case of the RS effect. The typical angular scale of lensing is several arcminutes.

These angles, however, are not directly observable; we would rather calculate the dispersion of the relative angular separation θ , which is defined as

$$\sigma_{\text{gl}}(\theta) \equiv \frac{1}{\sqrt{2}} \langle |\delta\theta_A - \delta\theta_B|^2 \rangle_{\theta}^{\frac{1}{2}}. \quad (34)$$

σ_{gl} is, like the case of the RS effect, proportional to $\sqrt{F_0}$. The values of $\sigma_{\text{gl}}(\theta)$ for each shell and their sum are computed just like the computation of $C_{\text{RS}}(\theta)$ in §3. Figure 10 shows a plot of $[\sigma_{\text{gl}}(\theta)/\theta]_{\theta=0.01\text{arcmin}}$ for each shell. Voids at $z \approx 50$ make the largest contribution to the CMB anisotropy: due to the factor W in equation (32), no effect arises from voids on the LSS, contrary to the case of the RS effect.

The values of $\sigma_{\text{gl}}(\theta)/\theta$ for the three models are presented in Figure 11. The results for Models (i) and (ii) indicate that the dependence on the formation time z_f is not so strong, as above. We also note that the results are similar to the previous results for a CDM model (Seljak 1996; Martínez-González, Sanz & Cayón 1997), though models and methods are quite different. The lensing effect for Model (iii) is not so large as that in Model (i) or (ii), though the RS effect is maximal in Model (iii) as shown in Figure. 8(c). This difference stems from the dependence of each effect on the void scale: as equations (14) and (33) shows, $\delta T/T|_{\text{RS}}$ is proportional to $(H_0 R_0)^{5/2}$, while $\sqrt{\langle |\delta\theta|^2 \rangle}$ is proportional to $(H_0 R_0)^{3/2}$.

Once $\sigma_{\text{gl}}(\theta)$ is obtained, we can calculate the lensing effect on the CMB fluctuations. Here we adopt the approximate formula of Seljak (1996) for the lensed correlation function:

$$\tilde{C}(\theta) = \frac{1}{2\pi} \int_0^\infty l dl e^{-\sigma_{\text{gl}}^2(\theta)l^2/2} C_l J_0(l\theta). \quad (35)$$

An example of the CMB anisotropy spectrum including lensing is presented in Figure 12(a). Here we plot $l(l+1)C_l$ versus l in linear scales in accordance with Seljak (1996). As Seljak (1996) and Martínez-González et al. (1997) showed for a CDM model, the lensing effect is to slightly smooth the main features appearing in the spectrum. To see the dependence on R_0 and z_t , we show the relative changes of the spectrum due to lensing for several cases in Figure 12(b), (c). We find that the lensing effect has a weak dependence on the formation time. That is, even if nonlinear voids exist from the recombination, they do not change the CMB anisotropy significantly. This feature is in contrast with that of the RS effect.

6. Summary and Discussions

We have studied the effect of a void network on the CMB anisotropy for TV’s model, where many voids are distributed in the Einstein-de Sitter background. In particular, we have examined how the CMB anisotropy spectrum affected by the RS effect, the SW effect, and the gravitational lensing effect.

Although the RS effect is negligible in conventional scenarios of structure formation like a CDM model, it can be appreciable if primordial voids exist already at recombination. In such a case, the SW effect of voids lying on the LSS is also important, and hence we have compared the two effects for several models. In most cases the SW term is larger than the RS term for $l \lesssim 1000$; however, if there are voids with the present radius $R_0 \gtrsim 60h^{-1}\text{Mpc}$, or equivalently, $r_v(t_{\text{LSS}}) \gtrsim 15h^{-1}\text{Mpc}$ on the LSS, both effects are comparable. Moreover, RS is the dominant effect on small scales.

For the SW effect of voids, Amendola, Baccigalupi & Occhionero (1998) and Baccigalupi (1998) argued that non-Gaussianity is large and it may give rise to ordered patterns in the CMB anisotropy field. For the RS effect, on the other hand, the deviation from Gaussianity depends on the number density of voids, or the volume fraction F_0 . If F_0 is so small as in Model (iii), the main contribution to the RS effect is made by a few voids near the LSS; then similar characteristic patterns may appear on the CMB map. On the other hand, if F_0 is of order unity as in Model (i) or (ii), the RS effect is generated by many (typically, more than ten) voids. In this case the central limit theorem implies that Gaussian statistics is a good approximation for the RS term itself; however, non-Gaussianity of the SW term exists and is dominant. It needs further investigation to clarify Gaussian/non-Gaussian feature of the RS effect more quantitatively.

As for gravitational lensing, the effect of nonlinear voids has not been investigated so far. Our present work is the first trial of that investigation without any approximation for nonlinearity nor

relativistic effect. We have shown how the primary anisotropy is smoothed out for some values of the void radius R_0 and of the formation time z_f . We have found that our results are similar to those for a CDM model (Seljak 1996; Martínez-González, Sanz & Cayón 1997).

Our results as a whole suggest that, if the real universe is filled with nonlinear voids, they make some appreciable effects on the CMB anisotropy. Those effects are expected to give some constraints on the configuration or origin of voids, particularly on the inflationary models in which primordial bubbles are nucleated, with the next generation of CMB satellites.

Acknowledgments

We thank Paul Haines for reading the manuscript. Numerical Computation of this work was carried out at the Yukawa Institute Computer Facility. N. Sakai was supported by JSPS Research Fellowships for Young Scientists. This work was supported partially by the Grant-in-Aid for Scientific Research Fund of the Ministry of Education, Science and Culture (No.9702603, No.09740334, and No.09440106).

A. On Double Lorentz Transformation

In this Appendix we show the equations of the double “Lorentz transformation” (5) can be derived exactly from a general coordinate transformation in a curved spacetime. Here we demonstrate the transformation at $t = t_1$ and omit the subscript 1.

First, we have to introduce another coordinate system which overlaps both the Einstein-de Sitter background and the Minkowski region. We adopt a Gaussian normal coordinate system $(\tau, n, \theta, \varphi)$ in which $n = 0$ represents the world-hypersurface of the shell. τ is chosen to be the proper time of the shell. i.e., the 3-metric at $n = 0$ is give by

$$ds^2 = -d\tau^2 + R^2(\tau)(d\theta^2 + \sin^2 \theta d\varphi^2). \quad (\text{A1})$$

The coordinate transformation of the 4-momentum k^μ at $n = 0$ from the Einstein-de Sitter frame $\{x_{\text{EdS}}^\mu\}$ to the Gaussian normal frame $\{y_{\text{GN}}^\nu\}$ is given by

$$k_{\mu}^{\text{GN}} = \frac{\partial x_{\text{EdS}}^\nu}{\partial y_{\text{GN}}^\mu} k_{\nu}^{\text{EdS}}. \quad (\text{A2})$$

It is easy to find

$$\frac{\partial t}{\partial \tau} = \gamma, \quad \frac{\partial r}{\partial \tau} = \frac{\gamma v}{a}, \quad (\text{A3})$$

and Sakai & Maeda (1993) obtained

$$\frac{\partial t}{\partial n} = \gamma v, \quad \frac{\partial r}{\partial n} = \frac{\gamma}{a}. \quad (\text{A4})$$

If we write the 4-momentum in each frame as

$$k_{\text{EdS}}^\mu = E \left(1, \frac{\cos \psi}{a}, \frac{\sin \psi}{ar}, 0 \right), \quad k_{\text{GN}}^\mu = E'' \left(1, \cos \psi'', \frac{\sin \psi''}{R}, 0 \right), \quad (\text{A5})$$

equation (A2) reduces

$$E'' = E\gamma(1 + v \cos \psi), \quad E'' \cos \psi'' = E\gamma(v + \cos \psi). \quad (\text{A6})$$

This is nothing but the expression of a usual Lorentz transformation. If we also carry out the coordinate transformation of the 4-momentum from the Gaussian normal frame to the Minkowski frame in the similar way, the expression of the double Lorentz transformation (5) is obtained.

B. Derivation of Thin Lens Equation

Here we derive the lens equation (32) from null geodesic equations. As depicted in Figure 1, we introduce a vector basis, $\{\mathbf{n}(\alpha), \mathbf{l}(\alpha)\}$, in the two-dimensional comoving space, and denote each position by a vector symbol \mathbf{r} . The trajectory of a photon in a homogeneous region is

$$\mathbf{r}_2 - \mathbf{r}_0 = \int_{t_2}^{t_0} \frac{dt}{a} \mathbf{n} = 3t_0(1 - \sqrt{a_2})\mathbf{n}, \quad (\text{B1})$$

$$\mathbf{r}_{\text{LSS}} - \mathbf{r}_1 = \int_{t_1}^{t_{\text{LSS}}} \frac{dt}{a} (\cos \delta \alpha \mathbf{n} + \sin \delta \alpha \mathbf{l}) = 3t_0 \left[(\sqrt{a_1} - \sqrt{a_{\text{LSS}}}) (\mathbf{n} + \delta \alpha \mathbf{l}) + O(\zeta^3) \right], \quad (\text{B2})$$

where we have expanded the equations with a dimensionless parameter,

$$\zeta \equiv \frac{r_2}{3t_0}. \quad (\text{B3})$$

To get the last equality of (B2), we have used the facts that $\delta \alpha$ is of order $(H_2 R_2)^2$ and that $H_2 R_2$ is of order ζ . Explicitly, the geodesic between \mathbf{r}_0 and \mathbf{r}_2 says equation (28) and

$$H_2 R_2 = \frac{2\zeta}{1 - d \cos \alpha / 3t_0 + \zeta \cos \psi_2}, \quad (\text{B4})$$

and hence equation (8) is rewritten as

$$\delta \alpha = \frac{8q\sqrt{1-q^2}}{(1 - d \cos \alpha / 3t_0)^2} \zeta^2 + O(\zeta^3) \quad \text{with} \quad q \equiv \frac{d}{r_2} \sin \alpha. \quad (\text{B5})$$

As for $\mathbf{r}_1 - \mathbf{r}_2$, we obtain

$$\mathbf{r}_1 - \mathbf{r}_2 = [r_1 \cos(\delta + \psi_1) + r_2 \cos \psi_2] \mathbf{n} + [r_1 \sin(\delta + \psi_1) - r_2 \sin \psi_2] \mathbf{l}. \quad (\text{B6})$$

In order to expand $\delta + \psi_1$, r_1 and $\sqrt{a_1}$ with ζ (or $H_2 R_2$), we use the relations

$$H_1 R_1 = H_2 R_2 - (3\beta - 1) \cos \psi_2 (H_2 R_2)^2 + \frac{3}{2} (3\beta - 1) \left[\left(\beta - \frac{2}{3} \right) \cos^2 \psi_2 + \beta \right] (H_2 R_2)^3 + O\left((H_2 R_2)^4 \right), \quad (\text{B7})$$

$$\psi_1 = \psi_2 + 3\beta H_2 R_2 \sin \psi_2 + O\left((H_2 R_2)^2\right), \quad (\text{B8})$$

which are found in the derivation of TV’s formula (7) and (8). Then we obtain

$$\mathbf{r}_1 - \mathbf{r}_2 = r_2(2 \cos \psi_2 - 3\beta H_2 R_2)\mathbf{n} + 3t_0 O(\zeta^3) = 3t_0[(\sqrt{a_2} - \sqrt{a_1})\mathbf{n} + O(\zeta^3)]. \quad (\text{B9})$$

Equation (B9) tells us that, although a photon is bent inside the void, the deviation is of order ζ^3 . From equations (B1)-(B4), (B9), and the relation,

$$\sqrt{a_1} = \sqrt{a_2} + O(\zeta) = 1 - \frac{d \cos \alpha}{3t_0} + O(\zeta), \quad (\text{B10})$$

we find

$$\begin{aligned} \mathbf{r}_{\text{LSS}} - \mathbf{r}_0 &= 3t_0 \left[(1 - \sqrt{a_{\text{LSS}}})\mathbf{n} + \left(1 - \frac{d \cos \alpha}{3t_0} - \sqrt{a_{\text{LSS}}}\right) \delta\alpha \mathbf{l} + O(\zeta^3) \right] \\ &= (\mathbf{r}_{\text{LSS}} - \mathbf{r}_0)_b + (d_{\text{LSS}} - d \cos \alpha) \delta\alpha \mathbf{l} + 3t_0 O(\zeta^3), \end{aligned} \quad (\text{B11})$$

where the subscript b denotes a background unperturbed quantity. We thus reach equation (32), i.e.,

$$\delta\theta \equiv \frac{\mathbf{r}_{\text{LSS}} - \mathbf{r}_{\text{LSS},b}}{d_{\text{LSS}}} = \frac{d_{\text{LSS}} - d \cos \alpha}{d_{\text{LSS}}} \delta\alpha \mathbf{l} + O(\zeta^3). \quad (\text{B12})$$

This result provides us a simple description: as long as we look at the leading terms of ζ , a void can be regarded to be a “thin lens” with a scattering angle $\delta\alpha$.

REFERENCES

- Amendola, L., Baccigalupi, C., Konoplick, R., Occhionero, F., & Rubin, S. 1996, Phys. Rev. D, 54, 7199
- Amendola, L., Baccigalupi, & Occhionero, F., 1998, ApJ, 492, L1
- Arnau, J.V., Fullana, M.J., Monreal, L., & Saez, D. 1993, ApJ, 402, 359
- Baccigalupi, C. 1998, ApJ, 496, 615
- Baccigalupi, C., Amendola, L., Fortini, P., & Occhionero, F. 1997, Phys. Rev. D, 56, 4610
- Baccigalupi, C., Amendola, L., & Occhionero, F. 1997, MNRAS, 288, 387
- Bertschinger, E. 1985, ApJS, 58, 1
- Blanchard, A., & Schneider, J. 1987, A&A, 184, 1
- Cayón, C., Martínez-González, E., & Sanz, J.L. 1993a, ApJ, 403, 471
- Cayón, C., Martínez-González, E., & Sanz, J.L. 1993b, ApJ, 413, 10

- Cole, S., & Efstathiou, G. 1989, MNRAS, 239, 195
- da Costa, L.N. et al. 1994, ApJ, 424, L1
- El-Ad, H., & Piran, T. 1997, astro-ph/9702135.
- El-Ad, H., Piran, T., & da Costa, L.N. 1996, ApJ, 462, L13
- El-Ad, H., Piran, T., & da Costa, L.N. 1997, MNRAS, 287, 790
- Fukushige, T., Makino, J., & Ebisuzaki, T. 1994, ApJ, 436, L107
- Fullana, M.J., Arnau, J.V., & Saez, D. 1996, MNRAS, 280, 1180
- Geller M.J., & Huchra J.P. 1989, Science, 246, 897
- Hu, W., Sugiyama, N., & Silk, J. 1997, Nature, 386, 37
- Kashlinsky, A. 1988, ApJ, 331, L1
- La, D. 1991, Phys. Lett. B, 265, 232
- Liddle, A.R., & Wands, D. 1991, MNRAS, 253, 637
- Linder, V.E. 1990a, MNRAS, 243, 353
- Linder, V.E. 1990b, MNRAS, 243, 362
- Maeda, K., & Sato, H. 1983, Prog. Theor. Phys., 70, 772
- Martínez-González, E., & Sanz, J.L. 1990, MNRAS, 247, 473
- Martínez-González, E., Sanz, J.L., & Cayón, C. 1997, ApJ, 484, 1
- Martínez-González, E., Sanz, J.L., & Silk, J. 1990, ApJ, 355, L5
- Mészáros, A. 1994, ApJ, 423, 19
- Mészáros, A., & Molnár, Z. 1996, ApJ, 468,
- Ochionero, F., & Amendola, L. 1994, Phys. Rev. D, 50, 4846
- Panek, M. 1992, ApJ, 388, 225
- Rees, M.J., & Sciama, D.W. 1968, Nature, 217, 511
- Sachs, R.K., & Wolfe, A.M. 1967, ApJ, 147, 73
- Sakai, N., & Maeda, K. 1993, Prog. Theor. Phys., 90, 1001
- Sasaki, M. 1989, MNRAS, 240, 415

Sato, H. 1985, *Prog. Theor. Phys.*, 73, 649

Seljak, U. 1996, *ApJ*, 463, 1

Shi, X., Widrow, L.M., & Dursi, L.J. 1996, *MNRAS*, 281, 565

Thompson, K.L., & Vishniac, E.T. 1987, *ApJ*, 313, 517

Tomita, K. 1989, *Phys. Rev. D*, 40, 3821

Tomita, K., & Watanabe, K. 1989, *Prog. Theor. Phys.*, 82, 563

Turner, M.S., Weinberg, E.J., & Widrow, L.M. 1992, *Phys. Rev. D*, 46, 2384

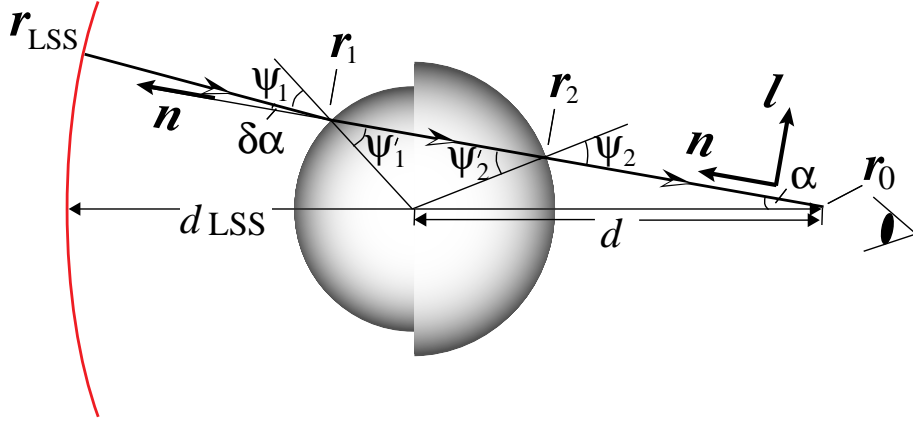


Fig. 1.— Cross section of a void on the $\varphi = \pi/2$ plane (TV’s model). We depict the trajectory of a photon from the LSS to an observer. The subscripts 1 and 2 denote quantities at the time the photon enters the void and at the time it leaves, respectively. The subscripts LSS and 0 denote quantities at the LSS and at present, respectively. Define α as the angle formed between the direction of observation and the direction of the void’s center, $\delta\alpha$ as the scattering angle of a photon, d as the comoving distance of the void’s center, and d_{LSS} as the comoving distance of the LSS. For Appendix B we denote each position by a vector symbol \mathbf{r} , and introduce a vector basis, $\{\mathbf{n}(\alpha), \mathbf{l}(\alpha)\}$, in the two-dimensional comoving space.

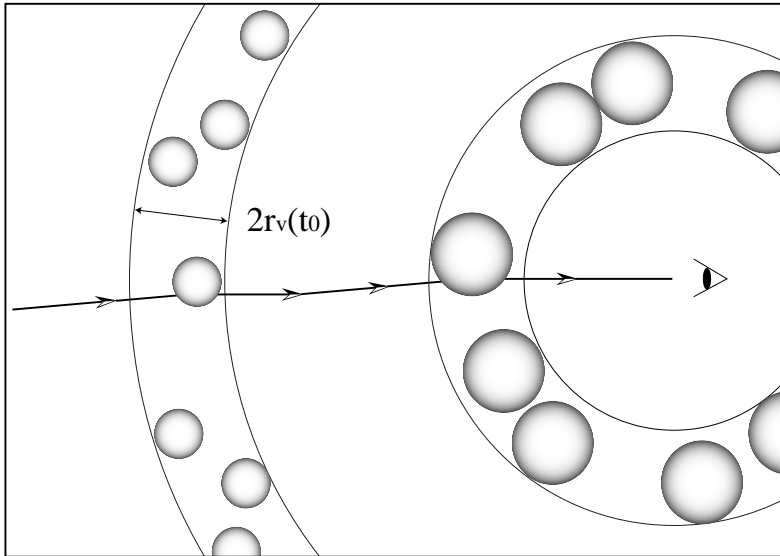


Fig. 2.— Schematic sketch of a void-network universe (TV’s model). Divide the universe into shells of comoving thickness $2r_v(t_0)$.

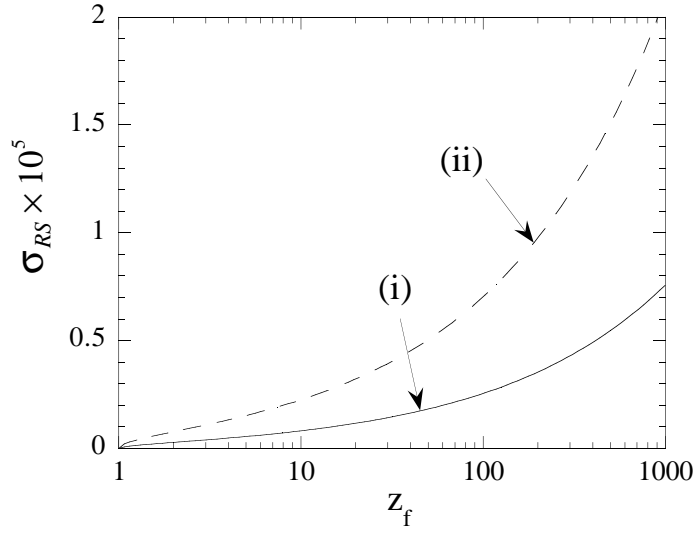


Fig. 3.— RS effect: plot of eq. (14) (TV’s results). We set $\beta = 0.13$ throughout this paper.

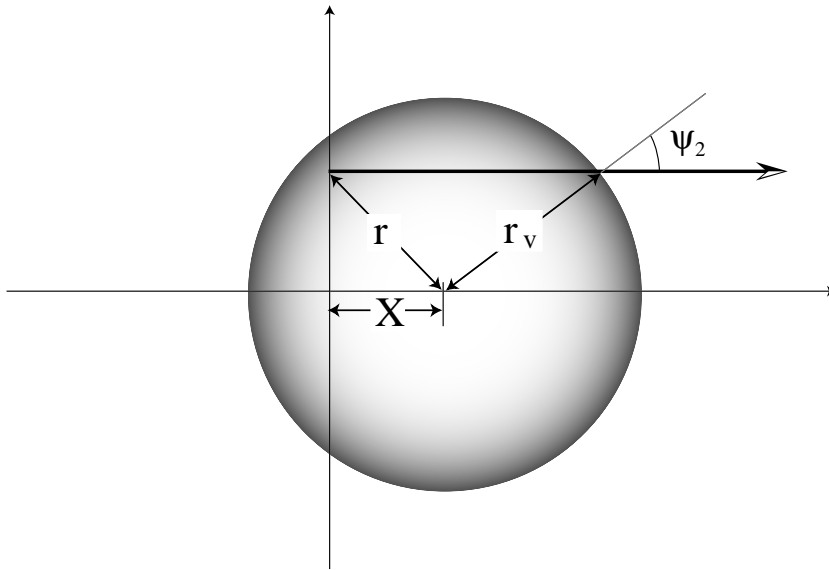


Fig. 4.— Void on the LSS. The vertical axis corresponds to the LSS, and X is defined as the distance between the void’s center and the LSS.

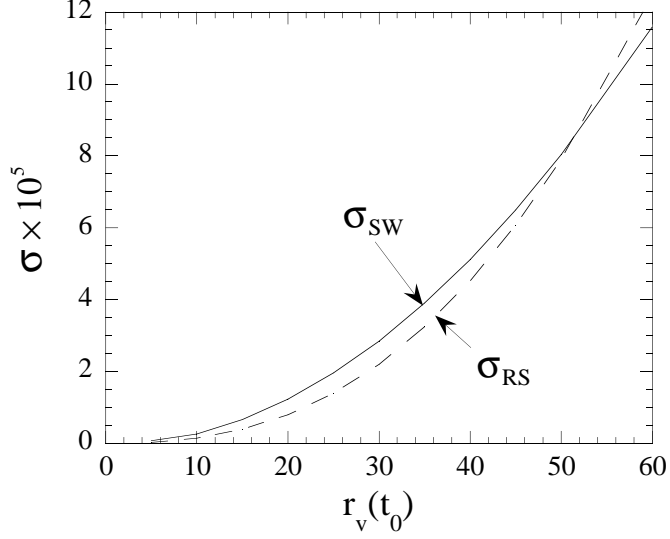


Fig. 5.— RS effect and SW effect: plot of σ_{RS} and σ_{SW} . v.s. $r_v(t_0)$. We set $F_0 = 50\%$.

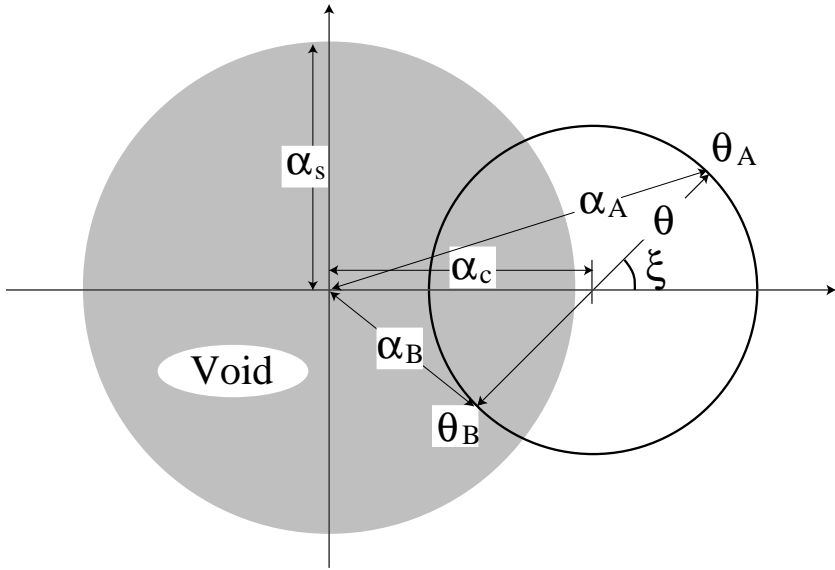


Fig. 6.— Projection of a void on the celestial sphere. Neglecting the curvature of the sphere in a local region around a void, we consider two light rays, which are labeled as θ_A and θ_B .

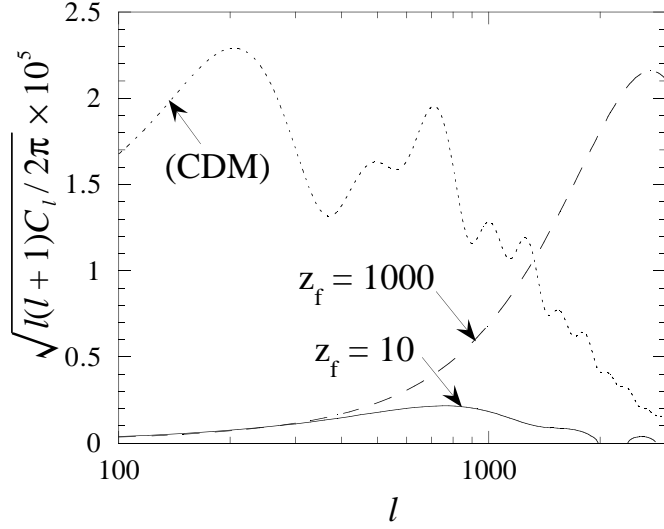
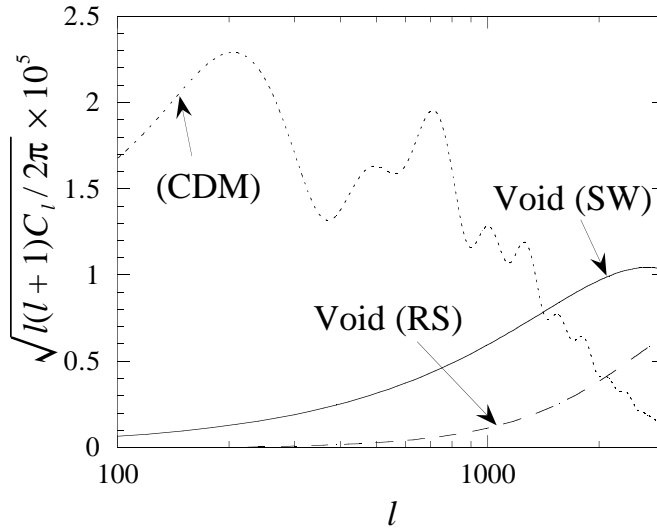
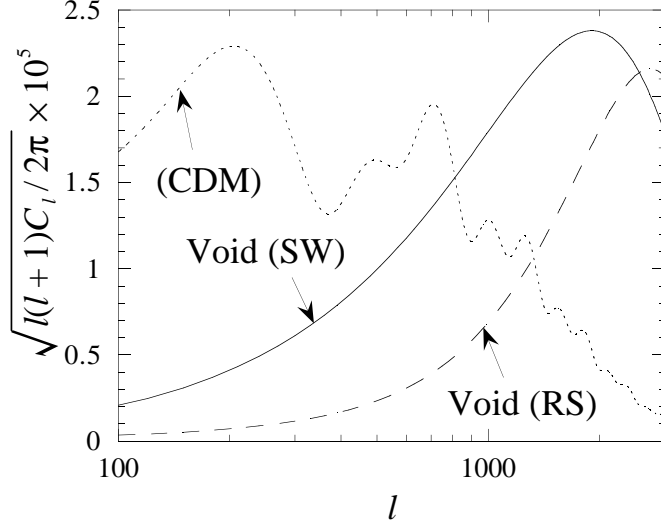


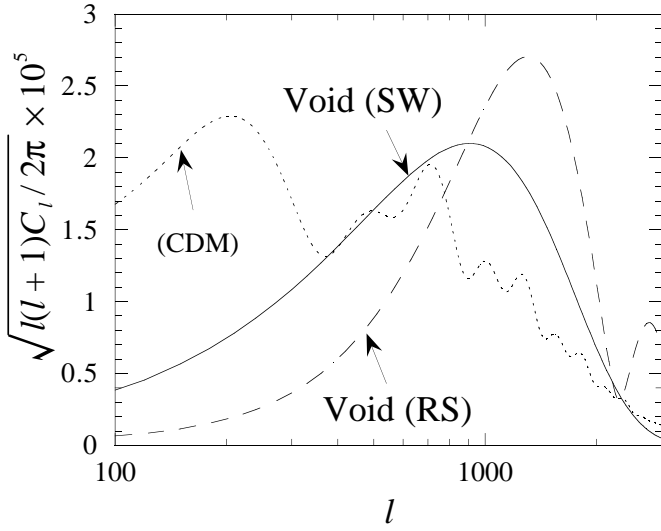
Fig. 7.— RS effect: plot of the CMB angular power spectrum $\sqrt{l(l+1)C_l}$ v.s. l for Model (ii). For reference, we also plot the values of C_l estimated for a CDM model.



(a)



(b)



(c)

Fig. 8.— RS effect and SW effect: plots of the CMB angular power spectrum $\sqrt{l(l+1)C_l}$ v.s. l . (a), (b), and (c) correspond to Models (a), (b), and (c), respectively. $z_f = 1000$.

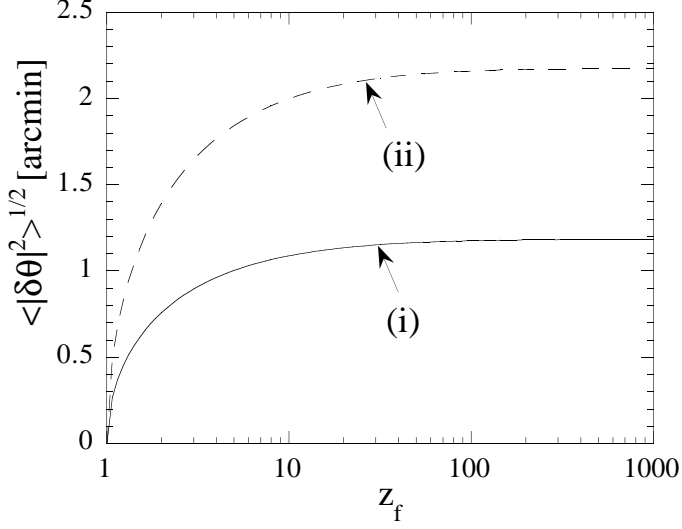


Fig. 9.— Lensing effect: plot of $\sqrt{\langle |\delta\theta|^2 \rangle}$ v.s. z_f .

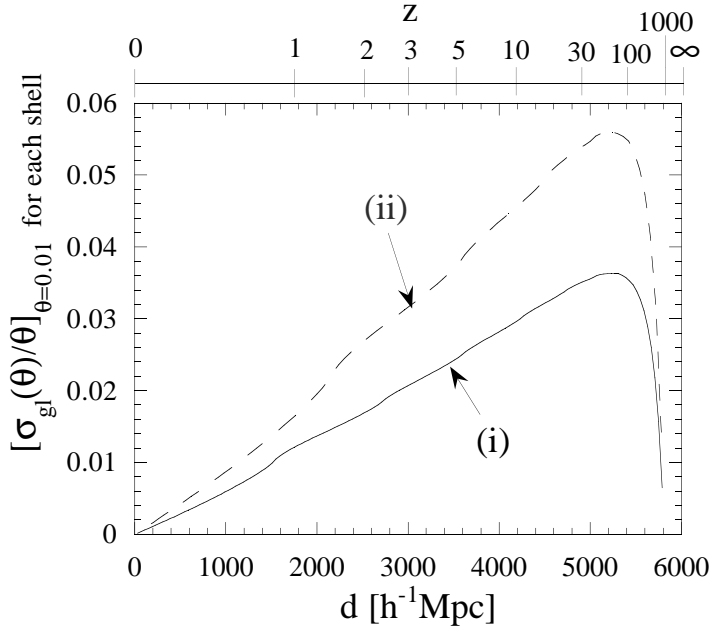


Fig. 10.— Lensing effect: contribution by voids in each shell. The abscissa is a position of shells in terms of $h^{-1}\text{Mpc}$ and z .

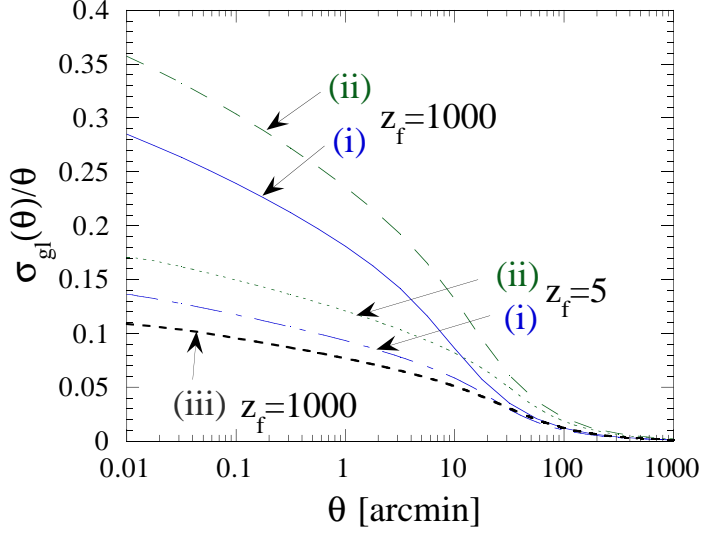
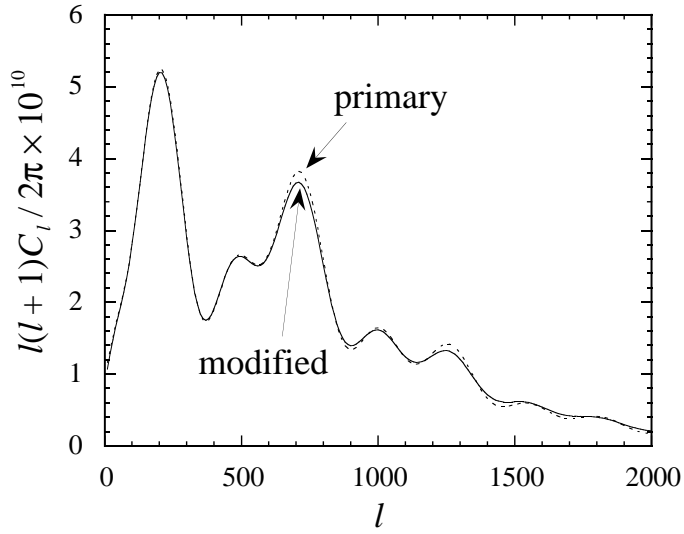
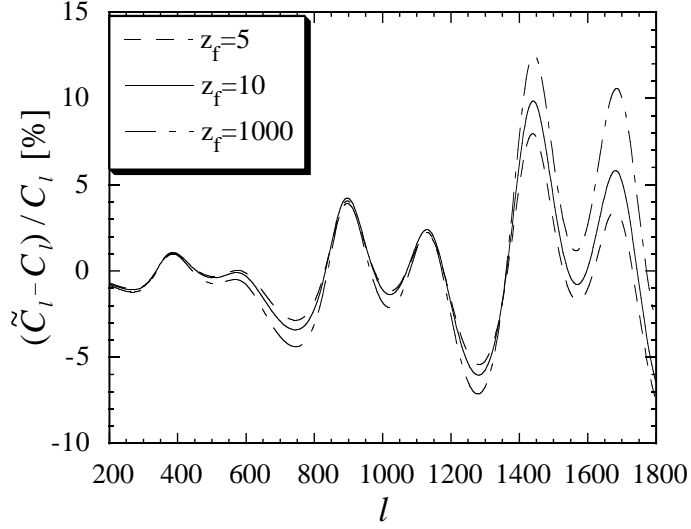


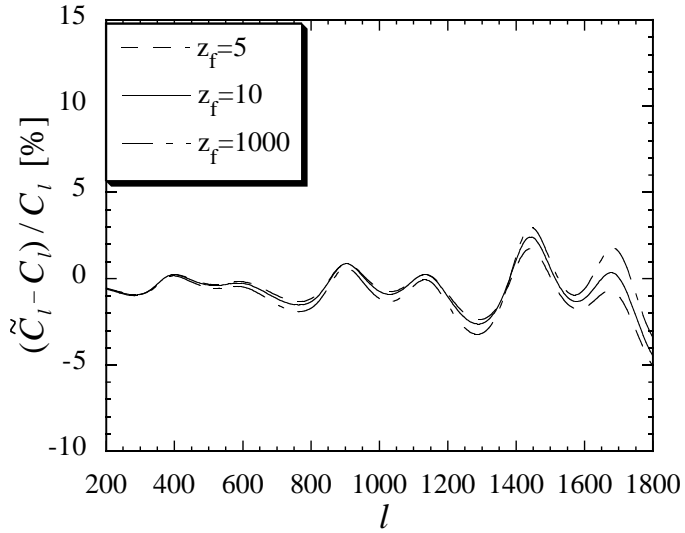
Fig. 11.— Lensing effect: plots of $\sigma_{\text{gl}}(\theta)/\theta$ v.s. θ . We show five examples: Model (i) with $z_f = 5$, (i) with $z_f = 1000$, (ii) with $z_f = 5$, (ii) with $z_f = 1000$, and (iii) with $z_f = 1000$,



(a)



(b)



(c)

Fig. 12.— Lensing effect. (a) shows plots of the CMB angular power spectrum $l(l+1)C_l$ v.s. l with lensing and without lensing for Model (ii). In (b) and in (c), respectively, the relative changes of the spectrum due to lensing for Model (i) and for Model (ii) are presented.